Hindawi
Advances in Materials Science and Engineering
Volume 2022, Article ID 9038912, 9 pages
https://doi.org/10.1155/2022/9038912

Research Article

Synthesis and Characterization of a Novel Bentonite Composite Superabsorbent Resin Based on Starch

Dongfang Li,[1] **Jing Guo**,[2] **Xinru Wang**,[3] **Lingnan Pei**,[4] **Wenjuan Li**,[1] **Yanxia Liu**,[1] **Yongchang Deng**,[3] **and Zhu Chen**[3]

[1]*School of Chemistry and Chemical Engineering, Jining Normal University, Ulanqab 012000, China*
[2]*College of Chemistry and Chemical Engineering, Inner Mongolia University, Hohhot 010021, China*
[3]*Hunan Key Laboratory of Biomedical Nanomaterials and Devices, Hunan University of Technology, Zhuzhou 412007, China*
[4]*School of Chemistry and Chemical Engineering, Liaoning Normal University, Dalian 116029, China*

Correspondence should be addressed to Dongfang Li; lidongfang1203@163.com and Zhu Chen; chenzhu@hut.edu.cn

Received 11 January 2022; Revised 18 April 2022; Accepted 9 May 2022; Published 21 June 2022

Academic Editor: Candido Fabrizio Pirri

A superabsorbent resin (SAR) is a functional polymer with a high water absorption capacity, which has been widely used in many fields. In this study, a modified aqueous solution polymerization process was adopted to synthesize a SAR. The optimum synthetical mass ratios of starch, bentonite, potassium persulfate ($K_2S_2O_8$), and N,N′-methylene-bis-acrylamide to acrylic acid (AA) were 7.14%, 3.57%, 0.29%, and 0.057%, respectively, and the neutralization degree of AA was 50%. The molecular structure and the surface morphologies of the SAR were confirmed using Fourier transform infrared spectroscopy and scanning electron microscopy. The SAR had a water absorbency of 1300 mL/g in distilled water and 56 mL/g in 0.9 wt.% NaCl solution. The water absorption rate reached 72.65% of the maximum water absorption in 1 hour and swelled to equilibrium in 4 hours. The water retention rate was 45.86% after heating and evaporation at 150°C for 1 hour. The moisture absorption rate reached 28.2% after 10 days of placement. The modified technology provides a new synthetic method for production of SARs, which is characterized by a lack of nitrogen protection, the direct use of raw AA and potato starch, a simplified synthesis process, substantially improved efficiency, and lower production costs.

1. Introduction

A superabsorbent resin (SAR) is a recently developed functional polymer material with strong hydrophilic groups, such as carboxyl and hydroxyl groups [1]. It is soluble in neither inorganic nor organic solvents and has a specific crosslinking degree (CD) and network structure [2]. SARs have a good adsorption performance, water retention capacity, pressure resistance, and heat resistance and have been used widely used in agriculture, forestry, and horticulture [3,4], industry [5–7], health supplies [8], and other fields [9–14].

However, most traditional water absorbent resins have poor degradability and are expensive [15]. To solve these problems, naturally available resources, such as polysaccharides and inorganic clay mineral, have been used recently as raw materials because of their renewability, biodegradability [16], and low cost. Introducing cheap mineral clay to modify SARs and synthesize composite SARs has become an important development direction [17]. Kaolin, bentonite, attapulgite, and many other clays have been used to synthesize SARs. Besides, starch is an extremely abundant natural resource and is used widely to synthesize SARs.

Traditionally, aqueous solution polymerization is commonly used to synthesize SARs, in which nitrogen and argon are essential to remove oxygen, and AA is purified before polymerization. Overall, these processes increase the complexity and cost of SAR synthesis. In this study, a novel SAR was investigated, which was based on potato starch, bentonite, and AA, with $K_2S_2O_8$ (potassium persulfate) as the initiator and N, N′-methylene-bis-

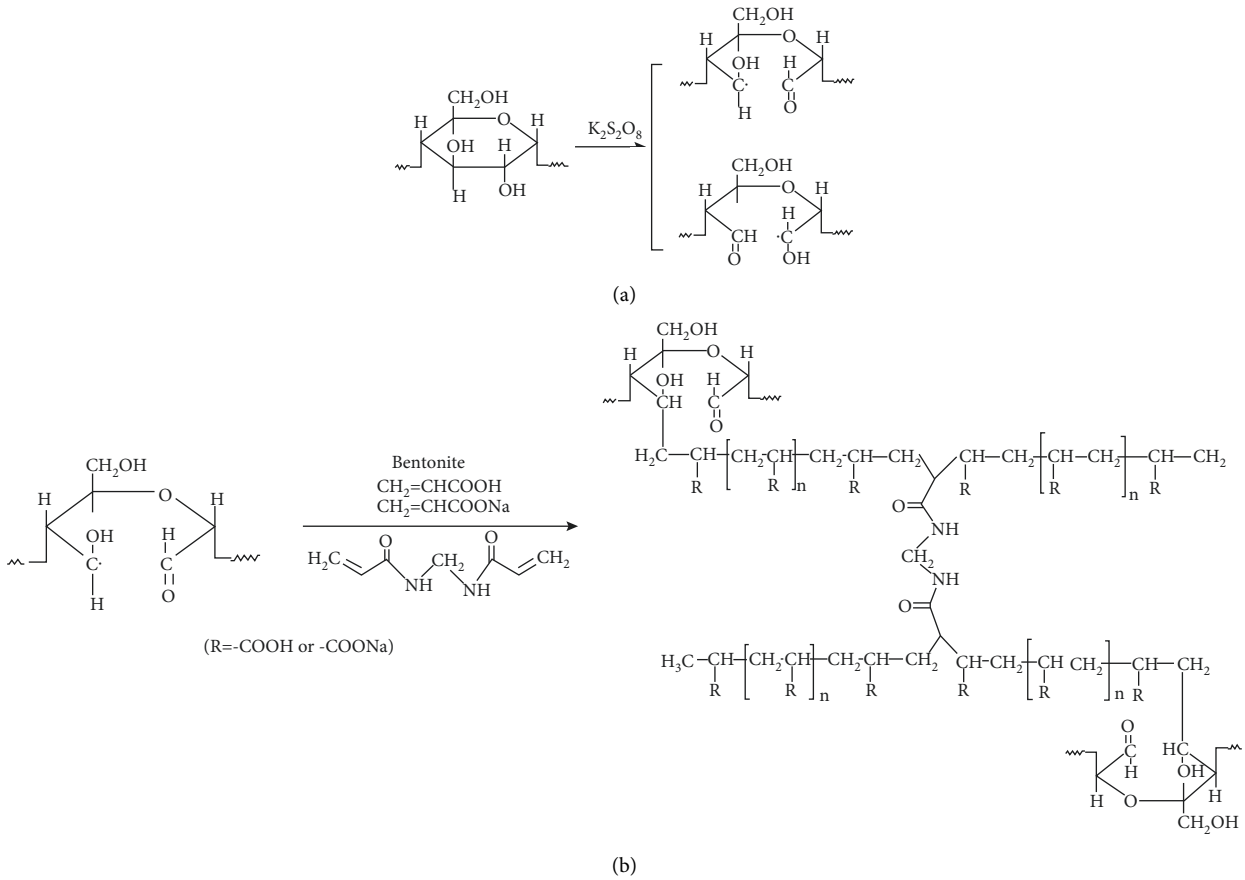

Figure 1: The synthesis mechanism of composite superabsorbent resin.

acrylamide (MBA) as the cross-linker. The modified method has no nitrogen protection during the polymerization process, with raw AA and potato starch being used directly. Also, the optimal ratio of raw materials and main influences of the reaction conditions for the composite SAR were investigated, and its structure and properties were evaluated.

2. Experimental

2.1. Materials. Potato starch was obtained from Inner Mongolia Minfeng Potato Industry Co., Ltd. (Inner Mongolia, China). Bentonite was obtained from Xinghe Zhongshun Bentonite Co., Ltd. (Inner Mongolia, China). Sodium hydroxide (NaOH) was purchased from Tianjin Xing'ao Chemical Reagent Technology Company (Tianjin, China). AA was supplied by Guangdong Tianhua Chemical Reagent Company (Guangdong, China). $K_2S_2O_8$ was purchased from Guangdong Bili Reagent Co., Ltd. (Guangdong, China). MBA was supplied by North China Special Chemical Reagent Development Center (Tianjin, China). Other agents were all of analytical grade and were used without further purification. All solutions were prepared using distilled water. All the experiments in this study had made three parallel experiments, each set of experiments had the same experimental results, and the data obtained were the average of the three experiments.

2.2. Pretreatment of Potato Starch and Bentonite. The potato starch and the bentonite were put into a mortar separately and ground into a uniform fine powder, dried in an air dry oven with the temperature of 35°C for 30 minutes to remove the moisture attached to their surfaces, and allowed to cool. In this study, the potato starch was not modified, and the bentonite did not need to be further purified.

2.3. Reaction Mechanism of the Composite SAR. The composite SAR was synthesized using a free radical polymerization reaction. Firstly, after being heated with the starch, $K_2S_2O_8$ initiates starch to produce free radicals (in Figure 1(a)). Secondly, the free radicals initiate AA polymerization and form starch-acrylic free radicals, which continue to polymerize with AA and cause chain propagation, and then a mesh macromolecule is formed by the crosslinking action of MBA (in Figure 1(b)) [18].

2.4. Synthesis of the Composite SAR. A certain amount of NaOH was dissolved in 25 mL of distilled water to prepare an NaOH solution to neutralize 20 mL AA, to which a certain amount of potato starch, bentonite, $K_2S_2O_8$, MBA, and 25 mL distilled water were added. The mixture was stirred for 30 minutes and placed in a water bath at an initial temperature of 35°C. Then, the water bath temperature was increased to 80°C within half an hour to facilitate the

polymerization reaction. The polymerization process could be completed in another 1.5 hours under these conditions. Subsequently, the synthetic product was taken out, cut into pieces, and dried in a drying oven at 70°C for 3 days, resulting in the composite SAR. Moreover, the SAR was milled and sifted through 20–40 meshes to prepare samples for performance testing.

2.5. Determination of Water/Salt Absorption. A sample (0.5 g) of the SAR was immersed in distilled water or NaCl solution. After the swelling equilibrium was reached, the unabsorbed water was filtered out. The water (salt) absorption (Q) was calculated using the following equation:

$$Q = \frac{V_1 - V_2}{m}, \quad (1)$$

where V_1 and V_2 are the volumes of added water and filtered water (mL), respectively, and m is the mass of the resin (g).

2.6. Determination of the Water Retention Rate at Different Temperatures. Samples of the SAR were poured into 1000 mL of distilled water. When the swelling equilibrium was reached, fully swollen hydrogels were obtained. After filtration, the weight of the hydrogels was measured after 1 hour drying at different temperatures. The water retention rate (R) was calculated as follows:

$$R = \frac{M_1}{M_0} \times 100\%, \quad (2)$$

where M_0 is the mass of the initial hydrogel (g) and M_1 is the mass of the hydrogel after drying (g).

2.7. Determination of the Moisture Absorption Rate. The temperature of the temperature and humidity test box was set at 25°C, and the humidity was set at 50%. After weighing, the dried composite SAR samples were placed in the constant temperature and humidity test box, and the moisture absorption was calculated at 0, 2, 4, 6, 8, and 10 days after SAR exposure. The moisture absorption rate (W) was calculated as

$$W = \frac{m_1 - m_0}{m_0} \times 100\%, \quad (3)$$

where m_0 is the mass of dry SAR (g) and m_1 is the mass of SAR after moisture absorption (g).

2.8. Characterization

2.8.1. Fourier Transform Infrared Spectroscopy (FTIR) Analysis. The structures and chemical bond compositions of the resin, the potato starch, and bentonite were analyzed using FTIR (TENSOR 27 FTIR, BRUKER company, Bremen, Germany). KBr pellets of the samples were used.

2.8.2. Scanning Electron Microscopy (SEM) Analysis. The surface morphology of the resin, potato starch, and bentonite were examined using the SEM (Sigma 300 field emission SEM, Carl Zeiss, Oberkochen Germany). The samples were coated with Au prior to SEM examination.

3. Results and Discussion

3.1. Effect of Synthesis Conditions on the Water Absorption of the Composite SAR

3.1.1. Effect of the Amount of Potato Starch. As shown in Figure 2(a), the water absorption of the SAR appeared to increase at first and then decrease as the amount of starch in the mixture increased. The largest water absorption value was obtained when the amount of potato starch was 1.5 g (the mass ratio of the potato starch to AA was 7.14%). It could be explained by the fact that starch is a basic skeleton to synthesize a SAR and provides active sites during the reaction. With the increase in the amount of potato starch, the number of active sites increases, which is beneficial to AA and its sodium salts to graft onto the starch, resulting in a gradual increase in water absorption. When the amount of starch was greater than 1.5 g, too many active centers were initiated on the starch chain, which could promote the formation of short branched chains, resulting in an increase in the crosslinking density. This would lead to the chain segment between the crosslinking points to become relatively short, and the network space between the crosslinking points becomes relatively small, which would result in the elastic expansion force of the network being correspondingly small, thus reducing the resin water absorption rate [22].

3.1.2. Effect of the Amount of Bentonite. The amount of bentonite could significantly affect the water absorption of the SAR (Figure 2(b)). When bentonite increased from 0.5 g to 0.75 g, the water absorbency of the SAR gradually increased, while this tendency decreased significantly after the amount of bentonite reached 1.0 g. Thus, the water absorbency of SAR was maximized with bentonite at 0.75 g (the mass ratio of bentonite to AA was 3.57%).

One explanation of this result is that the hydrophilic groups on the surface of bentonite (such as -OH) and in the SAR polymerization system (such as -$CONH_2$ and -COOH) could cooperate with each other, resulting in an increase in water absorption. At the same time, the hydrophilic groups can be used as crosslinking points during graft polymerization, which expands the network structure of the system. Therefore, the resin can absorb more water with increasing amounts of bentonite. However, when the amount of bentonite was over 0.75 g, the bentonite could not be evenly dispersed in the mixture, and the excess bentonite did not participate in the reaction but accumulated in a physical manner, which ultimately led to a large crosslinking point and a reduction in the extension degree of the molecular chain, making the network structure smaller. As a result, it would be difficult for water molecules to enter the SAR, thus reducing water absorption.

In addition, an increase in the amount of bentonite from 1.0 g to 1.5 g caused the surface of the resin to become adhesive, which is not conducive to water absorption. Therefore, considering the water absorption and the state of the resin, the optimal amount of bentonite was identified as 0.75 g.

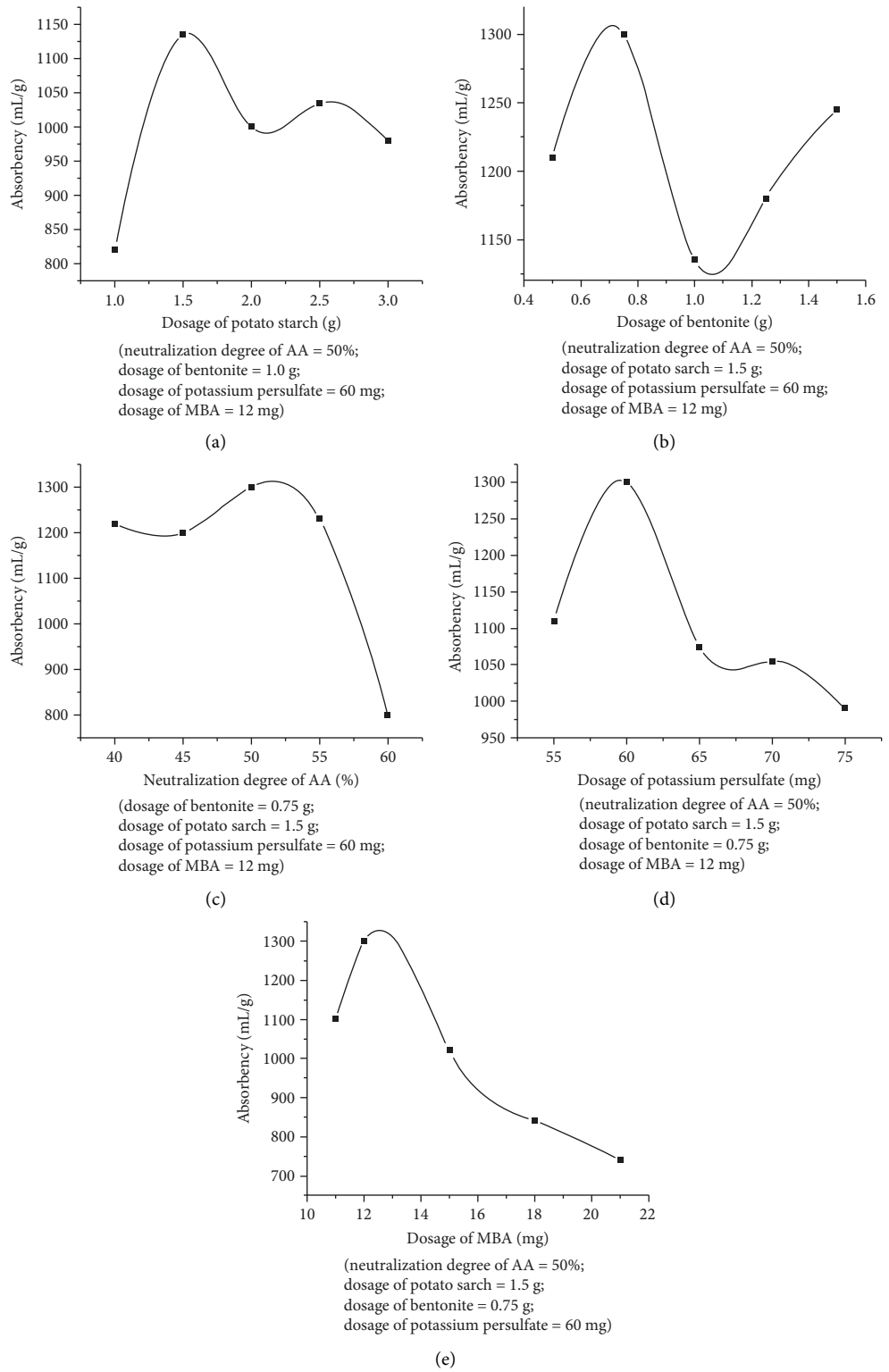

Figure 2: Effect of synthesis conditions on water absorption of superabsorbent resin. (a) The dosage of potato starch. (b) The dosage of bentonite. (c) The neutralization degree of acrylic acid. (d) The dosage of initiator. (e) The dosage of crosslinking agent.

3.1.3. Effect of the Neutralization Degree of AA. AA with different neutralization degrees can be obtained when the amount of NaOH changes. Thus, the effect of the neutralization degree of AA on the water absorption of the SAR was also tested (Figure 2(c)). We observed that the water absorption of the SAR increased at first and then decreased with the increase in the neutralization degree of AA, reaching a maximum when the neutralization degree of AA was 50%.

With the increasing degree of neutralization of AA, the ionization of carboxyl groups in the polymer chain increases,

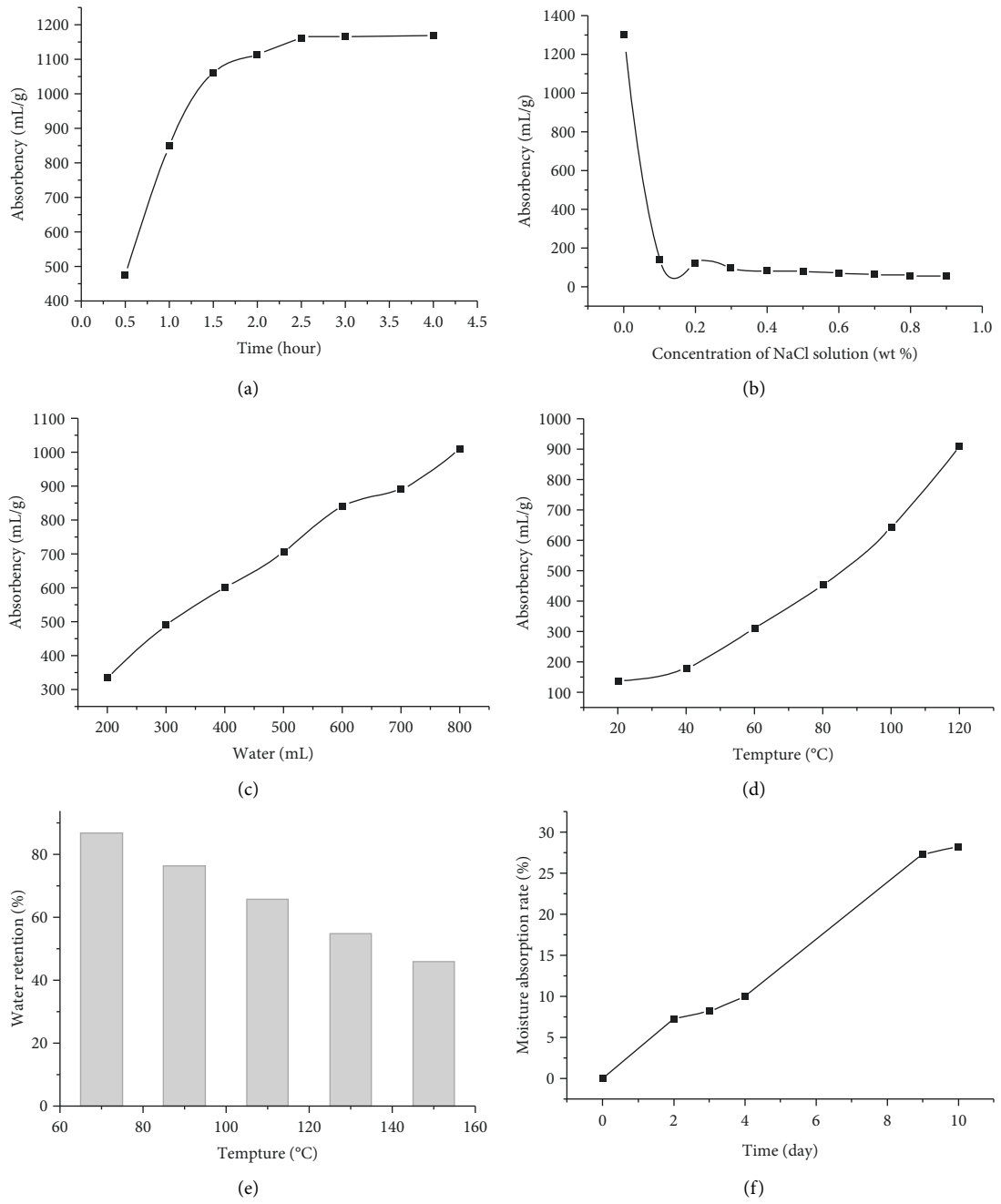

Figure 3: Properties of superabsorbent resin. (a) The water absorption rate. (b) Salt resistance. (c) Influence of water addition on water absorption. (d) Influence of temperature on water absorption. (e) The effect of temperature on water retention. (f) Moisture absorption.

resulting in an increase of repulsion, the network structure of the polymer product, and osmotic pressure; therefore, the water absorption of the SAR increases. However, when acrylic neutralization exceeds 50%, an excess of -COONa in the SAR results in an increase in water solubility of the resin, thereby decreasing the water absorption capacity of the resin [23].

3.1.4. Effect of the Amount of the Initiator. The relation between the water absorption of the SAR and the amount of the initiator $K_2S_2O_8$ was studied (Figure 2(d)). The result indicated the water absorption of the resin increased with increasing amounts of $K_2S_2O_8$, reaching a maximum when the amount of $K_2S_2O_8$ was 60 mg (the mass ratio of $K_2S_2O_8$ to AA was 0.29%), beyond which its water absorption capacity decreased.

When the amount of the initiator is low, fewer free radicals are produced and fewer active points are initiated, which will slow the rate of polymerization and reduce the CD of the three-dimensional network structure, consequently leading to low water absorption of the SAR. However, when the dose of the initiator is high, excessive free radicals are produced that accelerate the polymerization rate, causing an increase in the crosslinking density, a shortened chain length,

and a smaller network structure of the SAR. As a result, the water absorbing capacity of the SAR also decreases [24].

3.1.5. Effect of the Amount of the Crosslinking Activator (CA). The amount of MBA, which acted as a CA in synthesis of the SAR, also affected its water absorption capacity (Figure 2(e)). Water absorption was enhanced as the amount of MBA increased, reaching a maximum water absorption of 1300 mL/g when the amount of MBA was 12 mg (the mass ratio of MBA to AA was 0.057%).

Water absorbance of the resin is mainly dependent on the relative size of the network structure space and the CD in the system. When the amount of MBA was lower than 12 mg, the CD of the system gradually increased with increasing amounts of MBA, which resulted in the formation of an effective spatial network structure that increased the water absorption capacity. The CD of the system was optimal when the amount of MBA was 12 mg, which resulted in the formation of a suitable spatial network structure and maximized water absorption. However, when the amount of MBA was over 12 mg, the increase in crosslinking points in the SAR would enlarge the CD of the system and shrink the network structure of the resin. As a result, the SAR could not easily swell, and the water absorption capacity was reduced. Therefore, controlling the amount of MBA is one of the key factors in the synthesis of a high water absorbent resin.

3.2. Properties of the Novel SAR. As new functional polymer materials, SARs have become an indispensable material in the national economy, and it is very important to identify the properties of a newly developed SAR. Accordingly, water absorption, water retention, and moisture absorption of the SAR developed in the present study were evaluated.

3.2.1. Water Absorption. Water absorption is an important indicator to evaluate the application performance of an SAR. Thus, the effects of immersing time, salt solution concentration, water addition, and immersion temperature on the water absorption of the SAR were tested.

The effect of immersion time on water absorption by the SAR showed that the water absorption rate of the resin was fast, reaching 72.65% of the maximum water absorption in 1 hour and achieving swelling equilibrium in 4 hours (Figure 3(a)). This could be because the SAR is a kind of polymer electrolyte, and the internal groups of the SAR dissociate to produce ions when in contact with water. Accordingly, the ion concentration in the inside network is greater than that outside, generating osmotic pressure, and resulting in the diffusion of external water into the network [25]. With the continuous entry of external water, the hydrophilic groups inside the network further ionize, resulting in the increase in osmotic pressure between inside and outside the network and penetration of water molecules further. However, with the further increase of water molecules in the network, the ion concentration inside the network gradually decreases, so the ion concentration difference between inside and outside the network gradually decreases, which leads to a corresponding decrease in the osmotic pressure, ultimately reaching the swelling equilibrium of the water absorption of the SAR.

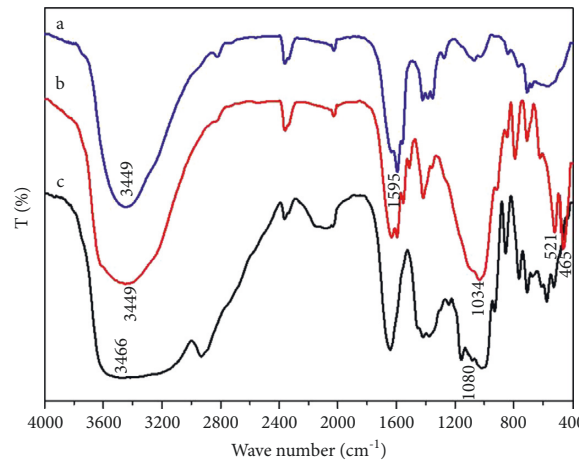

FIGURE 4: FTIR spectra of superabsorbent resin (a), bentonite (b), and potato starch (c).

The concentration of NaCl had a significant effect on the liquid absorption capacity of the SAR, and the water absorption decreased gradually as the NaCl concentration increased (Figure 3(b)). The water absorption of the SAR was 142 mL/g in 0.1 wt.% NaCl and 56 mL/g in 0.9 wt.% NaCl. The liquid absorption capacity of the SAR in NaCl solution was markedly less than that in distilled water. NaCl solution is a strong electrolyte that contains a large number of ions, resulting in a reduced ion concentration difference inside and outside the network structure, which reduces the osmotic pressure and hinders the entry of water molecules into the resin [26].

The water absorption of the SAR increased as the amount of water added increased (Figure 3(c)). The reason is that the higher the amount of water outside the resin, the greater the pressure it produces, which leads to increase water absorption of the resin. The water absorption of the SAR also increased as the immersion temperature increased (Figure 3(d)). This could be explained by the increase in the movement and spacing of water molecules between the chains of the SAR as the temperature rises, which results in an enlargement of the network space of the resin, thereby increasing water absorption [27].

3.2.2. Water Retention. Temperature had a significant influence on the water retention of the SAR (Figure 3(e)). The explanation is that some of the water molecules in the SAR are bound to the resin by hydrogen bonding and intermolecular van der Waals forces, and some are bound by the network structure [28]. Increasing the temperature intensifies the thermal movement of water molecules bound in the network structure, resulting in a decrease in the binding force of the resin to water molecules, causing the water retention of the SAR to decline significantly. The water retention rate of the SAR was still 45.86% after being heated and evaporated at 150°C for 1 hour, indicating that the resin had good water retention.

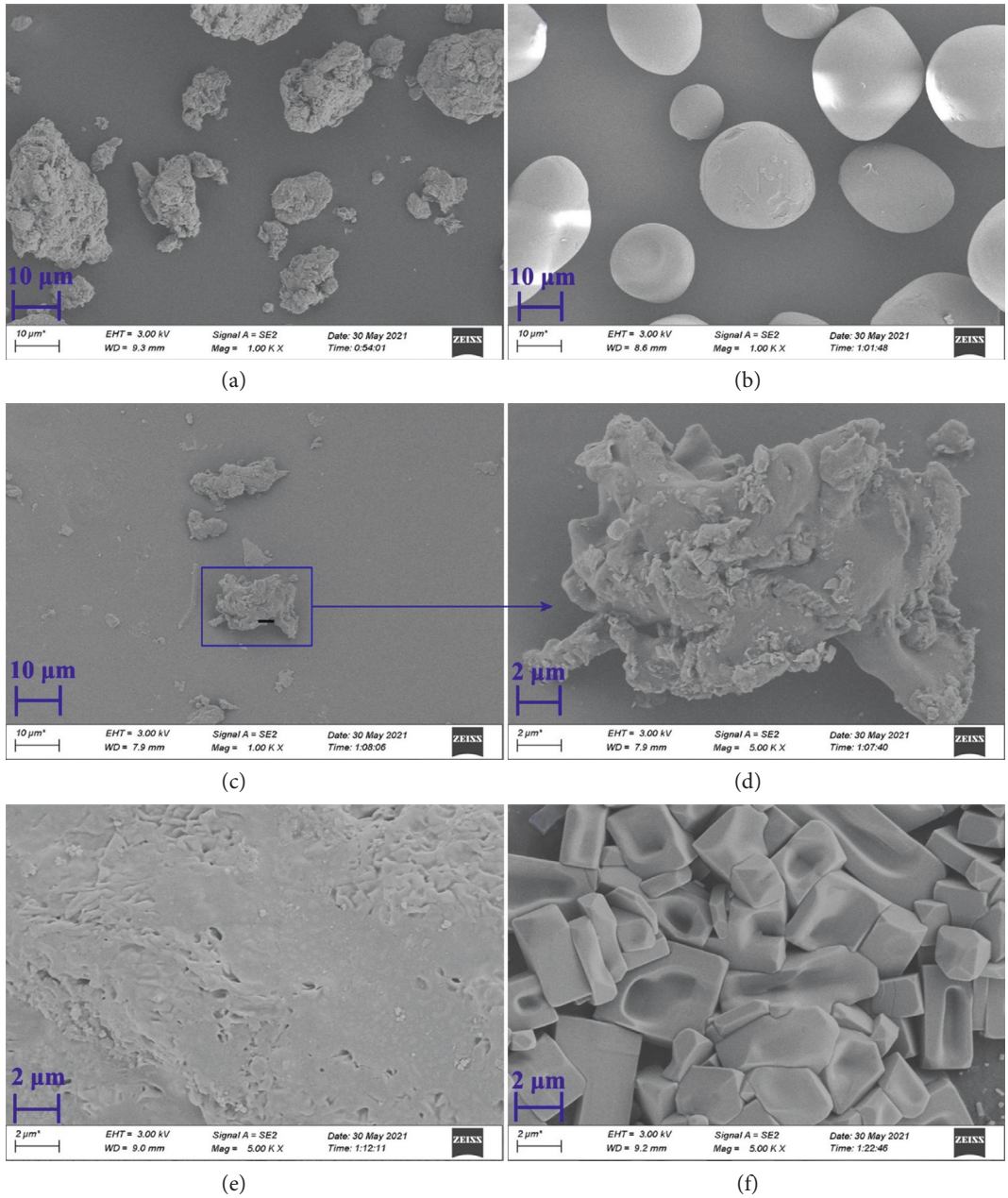

Figure 5: SEM images of (a) bentonite, (b) potato starch, (c, d) SAR, (e) SAR after absorbing distilled water and (f) SAR after absorbing salt water. SAR, superabsorbent resin; SEM, scanning electron microscope.

3.2.3. Moisture Absorption. As shown in Figure 3(f), the moisture absorption rate of the SAR continued to rise when it was left for 10 days. The moisture absorption rate was 7.27% after 2 days and 28.2% after 10 days. It could be explained by the fact that the SAR is a polymer gel with both a water absorbent function of the liquid state and a moisture absorption function of the gas state. Bentonite has strong moisture absorption, potato starch can swell in water, and acrylic acid can be mutually soluble with water. The SAR prepared from these raw materials contains a strong hydrophilic group, so it has good moisture absorption.

3.3. Characterization of the Novel SAR

3.3.1. FTIR Analysis. As shown in Figure 4, the telescopic vibration absorption peaks of -OH and $-COO^-$ in the SAR appeared at 3449 and 1595 cm^{-1}, respectively [29]. For potato starch, telescopic vibration absorption peaks were observed at 3466 cm^{-1} (-OH) and 1018 cm^{-1} (the α – 1,4-glucosidic bond in the potato starch chain). Comparison of the absorption peaks of potato starch and the SAR revealed that the telescopic vibration absorption peak of $-COO^-$ appeared in the spectrum of the resin, which suggested that AA and its salt had graft polymerized into the long chain of potato starch.

The FTIR spectrum of bentonite showed telescopic vibration absorption peaks at 3449 cm^{-1} (-OH in the structure of bentonite), 1634 cm^{-1} (-OH in interlayer water), and 1034 cm^{-1} (-O-Si in bentonite) and bending vibration absorption peaks of -O-Si at 521 cm^{-1} and 465 cm^{-1}. Comparison of the absorption peaks of bentonite and the SAR revealed that the telescopic vibration and bending vibration absorption peaks of -O-Si still existed in the spectrum of the resin, but the absorption peak was weak, indicating that the vibration dipole moment had changed, and bentonite had graft polymerized with AA and bound to the polymer chain of the resin through chemical bonds [30]. Thus, these findings showed that the highly absorbent resin was a crosslinked polymer formed by the polymerization of potato starch, bentonite, and AA.

3.3.2. Scanning Electron Microscopy Analysis. As shown in Figure 5, the original morphology of potato starch in the SAR no longer existed, indicating that potato starch had undergone relatively complete and uniform graft polymerization with AA and its sodium salt. Comparison of the original morphology of bentonite and the resin revealed some differences, which suggested that bentonite had graft polymerized with AA.

To investigate the effect of the ion concentration on the network structure of the SAR, the surface morphologies of the SAR after absorbing distilled water and after absorbing salt water were studied using the SEM. Comparison of the surface morphology of the two SARs revealed distinct differences. The surface morphology of the SAR after absorbing distilled water is covered with gullies and holes, which suggested that the resin had a large specific surface area and would have a high water absorption capacity [31]. The resin surface after absorbing salt solution was smooth and dense, which would reduce the surface area of the resin and thus decrease the liquid absorption capacity. The SEM results further demonstrated that the ions in solution affected the expansion of the network structure of the SAR.

4. Conclusions

A novel composite SAR was synthesized by aqueous solution polymerization using potato starch, bentonite, and AA as raw materials. The optimum synthetical mass ratios of starch, bentonite, potassium persulfate ($K_2S_2O_8$), and N, N′-methylene-bis-acrylamide to acrylic acid (AA) were 7.14%, 3.57%, 0.29%, and 0.057%, respectively, and the neutralization degree of AA was 50%. The SAR had a water absorbency of 1300 mL/g in distilled water. The results showed that the SAR synthesized using the modified method showed good water absorption, water retention, and moisturizing properties. The modified SAR synthetic method is characterized by a lack of nitrogen protection, the direct use of raw AA and potato starch, a simplified synthesis process, substantially increased efficiency, and lower production costs. The FTIR and SEM results showed that potato starch, AA, and bentonite were graft polymerized well, and the ions in solution could affect the expansion of the network structure of the SAR. In the related literature, the humidity of the experimental environment is not considered when determining the water retention rate of the resin. We will study its influence on the water retention rate of the SAR at different temperatures in the future.

Data Availability

The datasets used and/or analyzed during the current study are available from the corresponding author on reasonable request.

Conflicts of Interest

The authors declare that there are no conflicts of interest regarding the publication of this paper.

Acknowledgments

This work was supported by the Scientific Research Project of Colleges and Universities in Inner Mongolia Autonomous Region of China (Grant no. NJZY19240).

References

[1] Y. Wang, C. Wang, Y. Zhao, and P. Wang, "Effects of a superabsorbent resin with boron on bacterial diversity of peat substrate and maize straw," *BioMed Research International*, vol. 2018, 2018.

[2] W. Kong, Q. Li, J. Liu et al., "Adsorption behavior and mechanism of heavy metal ions by chicken feather protein-based semi-interpenetrating polymer networks super absorbent resin," *RSC Advances*, vol. 6, no. 86, pp. 83234–83243, 2016.

[3] L. Li, H. Zhang, X. Zhou, M. Chen, L. Lu, and X. Cheng, "Effects of super absorbent polymer on scouring resistance and water retention performance of soil for growing plants in ecological concrete," *Ecological Engineering*, vol. 138, pp. 237–247, 2019.

[4] Y. Yang, J. Wu, S. Zhao et al., "Effects of long-term super absorbent polymer and organic manure on soil structure and organic carbon distribution in different soil layers," *Soil and Tillage Research*, vol. 206, Article ID 104781, 2021.

[5] D. Shen, J. Jiang, M. Zhang, P. Yao, and G. Jiang, "Tensile creep and cracking potential of high performance concrete internally cured with super absorbent polymers at early age," *Construction and Building Materials*, vol. 165, pp. 451–461, 2018.

[6] J. Yang, Y. Guo, A. Shen, Z. Chen, X. Qin, and M. Zhao, "Research on drying shrinkage deformation and cracking risk of pavement concrete internally cured by SAPs," *Construction and Building Materials*, vol. 227, Article ID 116705, 2019.

[7] Z. Jin, H. Chang, F. Du, T. Zhao, Y. Jiang, and Y. Chen, "Influence of SAP on the chloride penetration and corrosion behavior of steel bar in concrete," *Corrosion Science*, vol. 171, Article ID 108714, 2020.

[8] N. Peng, Y. Wang, Q. Ye et al., "Biocompatible cellulose-based superabsorbent hydrogels with antimicrobial activity," *Carbohydrate Polymers*, vol. 137, pp. 59–64, 2016.

[9] Y. Tang, X. Wang, and L. Zhu, "Removal of methyl orange from aqueous solutions with poly(acrylic acid-co-acrylamide) superabsorbent resin," *Polymer Bulletin*, vol. 70, no. 3, pp. 905–918, 2013.

[10] L. Li, Z. Lin, L. Yu, W. Li, and G. Yang, "Self-assembling solid-state hydrogen source for drylands photocatalytic hydrogen production," *Journal of Materials Chemistry*, vol. 4, no. 41, pp. 15920–15928, 2016.

[11] A. Roshani, M. Fall, and K. Kennedy, "Impact of drying on geo-environmental properties of mature fine tailings pre-dewatered with super absorbent polymer," *International journal of Environmental Science and Technology*, vol. 14, no. 3, pp. 453–462, 2016.

[12] J. Geng, M. Chen, T. Shang, X. Li, Y. R. Kim, and D. Kuang, "The performance of super absorbent polymer (SAP) water-retaining asphalt mixture," *Materials*, vol. 12, no. 12, p. 1964, 2019.

[13] I. Anastopoulos, J. V. Milojković, K. Tsigkou et al., "A nappies management by-product for the treatment of uranium-contaminated waters," *Journal of Hazardous Materials*, vol. 404, Article ID 124147, 2021.

[14] T. Zou, T. Xu, H. Cui et al., "Super absorbent polymer as support for shape-stabilized composite phase change material containing $Na_2HPO_4{\cdot}12H_2O$-$K_2HPO_4{\cdot}3H_2O$ eutectic hydrated salt," *Solar Energy Materials and Solar Cells*, vol. 231, Article ID 111334, 2021.

[15] J. Xi and P. Zhang, "Application of super absorbent polymer in the Research of water-retaining and slow-release fertilizer," *IOP Conference Series: Earth and Environmental Science*, vol. 651, no. 4, Article ID 042066, 2021.

[16] Z. Ma, Q. Li, Q. Yue, B. Gao, X. Xu, and Q. Zhong, "Synthesis and characterization of a novel super-absorbent based on wheat straw," *Bioresource Technology*, vol. 102, no. 3, pp. 2853–2858, 2011.

[17] Y. Zhuo, J. Liu, F. Yang, Q. Li, and G. Xing, "Preparation and characterization of PVA/P(AA-AM) super absorbent polymer," *Integrated Ferroelectrics*, vol. 179, no. 1, pp. 166–172, 2017.

[18] R. J. Wang, L. W. Yang, H. D. Zhang, and T. J. Geng, "Synthesis of super absorbent resin from starch/bentonite," *Advanced Materials Research*, vol. 873, pp. 708–712, 2013.

[19] G. Lan, M. Zhang, Y. Liu et al., "Synthesis and swelling behavior of super-absorbent soluble starch-g -poly(AM-co -$NaAMC_{14}$ S) through graft copolymerization and hydrolysis," *Starch - Stärke*, vol. 71, Article ID 1800272, 2019.

[20] Y. Chen, Y.-f. Liu, H.-m. Tan, and J.-x. Jiang, "Synthesis and characterization of a novel superabsorbent polymer of N,O-carboxymethyl chitosan graft copolymerized with vinyl monomers," *Carbohydrate Polymers*, vol. 75, no. 2, pp. 287–292, 2009.

[21] Y. Zhang, L. Zhao, and Y. Chen, "Synthesis and characterization of starch-g -Poly(acrylic acid)/Organo-Zeolite 4A superabsorbent composites with respect to their water-holding capacities and nutrient-release behavior," *Polymer Composites*, vol. 38, no. 9, pp. 1838–1848, 2017.

[22] Q. Huo, D. Liu, J. Zhao, J. Li, R. Chen, and S. Liu, "Construction and water absorption capacity of a 3D network-structure starch-g-poly(sodium acrylate)/PVP Semi-Interpenetrating-Network superabsorbent resin," *Starch - Stärke*, vol. 69, no. 11-12, Article ID 1700091, 2017.

[23] W. Kong, Q. Li, X. Li, Y. Su, Q. Yue, and B. Gao, "A biodegradable biomass-based polymeric composite for slow release and water retention," *Journal of Environmental Management*, vol. 230, pp. 190–198, 2019.

[24] Y. Li, A. Sawut, G. Hou, M. He, and M. Yimit, "UV polymerization and property analysis of maleacylated methyl cellulose acrylic acid absorbent resin," *Polish Journal of Chemical Technology*, vol. 22, no. 2, pp. 34–41, 2020.

[25] H. Baloch, M. Usman, S. A. Rizwan, and A. Hanif, "Properties enhancement of super absorbent polymer (SAP) incorporated self-compacting cement pastes modified by nano silica (NS) addition," *Construction and Building Materials*, vol. 203, pp. 18–26, 2019.

[26] A. Rashidzadeh and A. Olad, "Slow-released NPK fertilizer encapsulated by NaAlg-g-poly(AA-co-AAm)/MMT super-absorbent nanocomposite," *Carbohydrate Polymers*, vol. 114, pp. 269–278, 2014.

[27] S. Xu, Y. Yin, Y. Wang, X. Li, Z. Hu, and R. Wang, "Amphoteric superabsorbent polymer based on waste collagen as loading media and safer release systems for herbicide 2, 4-D," *Journal of Applied Polymer Science*, vol. 137, no. 12, Article ID 48480, 2019.

[28] H. Mazi and B. Surmeli̇hi̇ndi̇, "Temperature and pH-sensıtıve super absorbent polymers based on modıfied maleıc anhydrıde," *Journal of Chemical Sciences*, vol. 133, no. 1, p. 10, 2021.

[29] N. Gawande and A. A. Mungray, "Superabsorbent polymer (SAP) hydrogels for protein enrichment," *Separation and Purification Technology*, vol. 150, pp. 86–94, 2015.

[30] P. Lertsarawut, T. Rattanawongwiboon, T. Tangthong et al., "Starch-based super water absorbent: a promising and sustainable way to increase survival rate of trees planted in arid areas," *Polymers*, vol. 13, no. 8, p. 1314, 2021.

[31] A. Sawut, M. Yimit, W. Sun, and I. Nurulla, "Photopolymerisation and characterization of maleylatedcellulose-g-poly(acrylic acid) superabsorbent polymer," *Carbohydrate Polymers*, vol. 101, pp. 231–239, 2014.